arXiv:hep-ph/0606063v2 12 Jun 2006

The phase diagram of neutral quark matter with pseudoscalar condensates in the color-flavor locked phase

Harmen J. Warringa[1, 2, *]
[1]*Department of Physics, Vrije Universiteit, De Boelelaan 1081, 1081 HV Amsterdam, The Netherlands*
[2]*Department of Physics, Norwegian University of Science and Technology, N-7491 Trondheim, Norway*

(Dated: February 2, 2008)

We calculate the phase diagram of color and electrically neutral quark matter in weak equilibrium using the NJL model at high baryon densities. We extend previous analyses by taking into account the possibility of formation of pseudoscalar meson condensates in the color-flavor locked (CFL) phase. We find that the kaon condensed phase (CFL-K^0) is preferred over the CFL phase at low temperatures. It is found that the CFL-K^0 phase contains no gapless modes. The results we have obtained should be of relevance for the modeling of compact stars.

I. INTRODUCTION

At sufficiently high baryon densities, massless three-flavor QCD is in a color-flavor locked (CFL) phase [1]. In the CFL phase the original $\mathrm{SU}(3)_L \times \mathrm{SU}(3)_R \times \mathrm{SU}(3)_c \times \mathrm{U}(1)_B$ symmetry of QCD is broken to $\mathrm{SU}(3)_{V+c}$ due to the formation of scalar diquark condensates. As a consequence all eight gluons become massive by the Anderson-Higgs mechanism. Furthermore the breakdown of chiral symmetry leads to the emergence of eight massless pseudoscalar excitations, similar to what happens in QCD at low baryon densities. Casalbuoni and Gatto have constructed a chiral effective theory for the CFL phase [2] that describes these massless excitations. In such a chiral effective theory the pseudoscalar excitations π^a are contained in a flavor octet chiral field $\Sigma = \exp(i\pi^a\lambda^a/f_\pi)$. Here f_π is the pion decay constant and the Gell-Mann matrices λ_a are normalized as $\mathrm{tr}\,\lambda_a\lambda_b = 2\delta_{ab}$, where $a = 1\ldots 8$. The field Σ transforms under $\mathrm{SU}(3)_L \times \mathrm{SU}(3)_R$ as $\Sigma \to U_L \Sigma U_R^\dagger$.

In the CFL phase with massless quarks the vacuum expectation value of the Σ field is equal to 1. However, finite quark masses and chemical potentials give rise to a potential for Σ [3, 4, 5]. Depending on the values of the chemical potentials and the current quark masses m_u, m_d and m_s the new ground state can have $\Sigma \neq 1$, which arises via an axial flavor transformation on the CFL ground state. In such a case one of the pseudoscalar meson fields obtains a vacuum expectation value [4]. Depending on the fields involved one speaks of pion or kaon condensation giving rise to the CFL-$\pi^\pm$, CFL-K^0 and CFL-K$^\pm$ phases [5, 6].

Using the chiral effective theory it was found that pseudoscalar condensation can occur if the chemical potential of the mesonic excitation exceeds the mass of the corresponding excitation. For the case $m_u = m_d$ the masses of the pionic and kaonic excitations (not to be confused with the masses m_π and m_K of the pion and kaon mesons) in the chiral effective theory for the CFL phase are respectively found to be [3] $M_\pi^2 = 2am_um_s$ and $M_\mathrm{K}^2 = a(m_u + m_s)m_u$. At asymptotically high densities $a = 3\Delta^2/(\pi^2 f_\pi^2)$ [3], where Δ is the CFL gap and the pion decay constant is given by $f_\pi^2 = (21 - 8\log 2)\mu^2/(36\pi^2)$. Here μ denotes one third of the baryon chemical potential. The chemical potentials of the pseudoscalar mesons are [6] $\mu_{\pi^+} = \mu_Q$,

$$\mu_{\mathrm{K}^+} = \mu_Q + \frac{m_s^2 - m_u^2}{2\mu}, \qquad \mu_{\mathrm{K}^0} = \frac{m_s^2 - m_d^2}{2\mu}, \quad (1)$$

where μ_Q is the chemical potential for electric charge. The chemical potentials of the antiparticles are the opposite of those above. The π^0 does not condense since its chemical potential vanishes [6]. The η and the η' excitation can however obtain a vacuum expectation value [7], but will not be taken into account in this article.

The parameters of the chiral effective theory analysis have to be matched to QCD, which only can be done accurately at extremely high baryon densities where perturbative QCD is applicable. However, it is interesting to know how matter behaves at non-asymptotic baryon densities, such as inside a compact star. Therefore it would be worthwhile to have an alternative analysis of pseudoscalar condensation in the color superconducting phases which could be reliable at intermediate baryon densities. The model we use for that purpose here is the Nambu–Jona-Lasinio (NJL) model (see [8] for a review). The NJL model has been applied to study the QCD phase diagram as a function of baryon chemical potential and temperature under compact star constraints [9, 10, 11] (see e.g. [12] for a review of compact stars). In this article we will extend the NJL model analysis of the phase diagram of Refs. [9, 10, 11] by including the possibility of pseudoscalar condensation in the color-superconducting phases. In this way we are able to obtain a more detailed phase diagram for quark matter under compact star constraints, that is electrically and color neutral matter in weak equilibrium. Earlier investigations of pseudoscalar condensation in the CFL phase using the NJL model have been performed in Refs. [13, 14]. The phase diagram of quark matter under compact star constraints was however not calculated in Refs. [13, 14]. Reasonable agreement between the chiral effective theory and

---

[*] Electronic address: harmen@tf.phys.ntnu.no

the NJL model approach to pseudoscalar condensation in the CFL phase was found in [13, 14]. This we will use as a justification to apply some of the outcomes of the chiral effective theory analysis.

This article is organized as follows. In Sec. II we discuss shortly the NJL model and the parameter choices. The details of the calculation are given in Sec. III. The reader only interested in the main results may go directly to Sec. IV in which the phase diagram of quark matter under compact star constraints is presented. We summarize and conclude in Sec. V.

II. THE NJL MODEL

In the NJL model, one treats the interaction between the quarks as a point-like quark color current-current interaction. We will use the following Lagrangian density

$$\mathcal{L} = \bar{\psi}\left(i\gamma^\mu\partial_\mu - \hat{m} + \hat{\mu}\gamma_0\right)\psi + \mathcal{L}_{\bar{q}q} + \mathcal{L}_{qq} + \mathcal{L}_{\mathrm{H}}, \tag{2}$$

where the quark-antiquark term, $\mathcal{L}_{\bar{q}q}$, the diquark interaction term, $\mathcal{L}_{qq}$, and the 't Hooft interaction term $\mathcal{L}_{\mathrm{H}}$ are defined below. We have suppressed the color (c), flavor (f), and Dirac (d) indices of the fermion fields ψ for notational simplicity. The mass matrix $\hat{m}$ is diagonal and contains the current quark masses. The matrix $\hat{\mu}$ is also diagonal in flavor space and contains the quark chemical potentials. In order to allow for electric and color neutralization [11, 15, 16, 17] we write

$$\hat{\mu} = \mu \mathbb{1}_c \otimes \mathbb{1}_f + \mu_Q \mathbb{1}_c \otimes Q + \mu_3 t_3 \otimes \mathbb{1}_f + \mu_8 t_8 \otimes \mathbb{1}_f, \tag{3}$$

where $Q = \mathrm{diag}(2/3, -1/3, -1/3)$. When we later on in Sec. III we introduce a electron (e) and muon (μ) gas, this choice will automatically enforce the weak equilibrium conditions, $\mu_{d,s} = \mu_u + \mu_{e,\mu}$. The color matrices corresponding to the color chemical potentials μ_3 and μ_8 are $t_3 = \mathrm{diag}(1, -1, 0)$ and $t_8 = \mathrm{diag}(1, 1, -2)/\sqrt{3}$. We use the metric $g^{\mu\nu} = \mathrm{diag}(+ - - -)$ and the standard Dirac representation for the γ-matrices. The quark-antiquark interaction part of the Lagrangian density is

$$\mathcal{L}_{\bar{q}q} = G\left[\left(\bar{\psi}\lambda_a\psi\right)^2 + \left(\bar{\psi}\lambda_a i\gamma_5\psi\right)^2\right]. \tag{4}$$

Here the matrices λ_a denote the 9 generators of U(3) and act in flavor space. They are normalized as $\mathrm{Tr}\,\lambda_a\lambda_b = 2\delta_{ab}$. To remind the reader, the antisymmetric flavor matrices λ_2, λ_5 and λ_7 couple up to down, up to strange and down to strange quarks, respectively. The diquark interaction term of the Lagrangian density is given by

$$\begin{aligned}\mathcal{L}_{qq} &= \frac{3}{4}G\left(\bar{\psi}t_A\lambda_B C i\gamma_5\bar{\psi}^T\right)\left(\psi^T t_A\lambda_B C i\gamma_5\psi\right) \\ &+ \frac{3}{4}G\left(\bar{\psi}t_A\lambda_B C\bar{\psi}^T\right)\left(\psi^T t_A\lambda_B C\psi\right),\end{aligned} \tag{5}$$

where $A, B \in \{2, 5, 7\}$ since only the interaction in the color and flavor antisymmetric triplet channel is attractive. The matrices t_a are the generators of U(3) and act in color space. Their normalization is $\mathrm{tr}\, t_a t_b = 2\delta_{ab}$. The charge conjugate of a field ψ is denoted by $\psi_c = C\bar{\psi}^T$ where $C = i\gamma_2\gamma_0$. The coupling strength $3G/4$ of the diquark interaction is fixed by the Fierz transformation (see for example Ref. [8]). However, some authors discuss the NJL model with a different diquark coupling constant (in Ref. [9] it was found that changing this coupling strength to G can have a non-negligible effect on the phase diagram). Finally, the 't Hooft interaction which models an additional breakdown of the axial U(1) symmetry due to instantons is given by [18]

$$\mathcal{L}_{\mathrm{H}} = -K\left[\mathrm{det}_f\bar{\psi}(1-\gamma_5)\psi + \mathrm{det}_f\bar{\psi}(1+\gamma_5)\psi\right]. \tag{6}$$

The results that will be presented below are obtained with the following choice of parameters [9, 19]

$$\begin{gathered} m_u = m_d = 5.5\ \mathrm{MeV}, \quad m_s = 140.7\ \mathrm{MeV} \\ G = 1.835/\Lambda^2, \quad K = 12.36/\Lambda^5, \quad \Lambda = 602.3\ \mathrm{MeV}. \end{gathered} \tag{7}$$

This choice of parameters gives the following parameters the realistic values [19] $m_\pi = 135.0$ MeV, $m_{\mathrm{K}} = 497.7$ MeV, $m_\eta = 514.8$ MeV, $m_{\eta'} = 957.8$ MeV, and $f_\pi = 92.4$ MeV. Moreover, it allows us to compare our results to the phase diagram obtained in [9], where only the scalar diquark condensates were taken into account.

III. CALCULATION OF THE PHASE DIAGRAM

To obtain the phase diagram of the NJL model, we introduce the chiral condensates

$$\sigma_u = \langle\bar{u}u\rangle, \quad \sigma_d = \langle\bar{d}d\rangle, \quad \sigma_s = \langle\bar{s}s\rangle, \tag{8}$$

and the scalar and pseudoscalar diquark condensates

$$\Delta^s_{AB} = \frac{3}{2}G\langle\psi^T t_A\lambda_B C\gamma_5\psi\rangle, \quad \Delta^p_{AB} = \frac{3}{2}G\langle\psi^T t_A\lambda_B C\psi\rangle. \tag{9}$$

We do not take into account the possibility of pion condensation or charged kaon condensation outside the CFL phase (e.g. the appearance of $\langle\bar{u}i\gamma_5 d\rangle$ and $\langle\bar{u}i\gamma_5 s\rangle$, condensates). Using the results of [20] this is in principle possible if $|\mu_Q| > m_\pi$ or $|\mu_Q| > m_{\mathrm{K}}$. Phase diagrams with these condensates have been investigated in Refs. [21, 22, 23, 24]. From Ref. [9] we conclude that electric neutralization gives values of $|\mu_Q|$ which are smaller than m_{K} making the occurrence of this type of kaon condensate unlikely. Electric neutralization allows for values $|\mu_Q|$ which are larger than m_π, but from the analysis of Ref. [24] it follows that for matter in weak equilibrium the phase with the pion condensate is not competing against color superconducting phases. This makes it in our opinion improbable that such a condensate arises in neutral quark matter at high baryon densities.

In the CFL phase with massless quarks the nonzero condensates are $\Delta^s_{22} = \Delta^s_{55} = \Delta^s_{77}$. In the more realistic situation of unequal quark masses and unequal chemical potentials the same condensates appear, but then they are no longer equal to each other. As was explained in the introduction the state with pseudoscalar condensation in the CFL phase can be obtained by an axial flavor transformation on the CFL state. In such a case $\psi \to \exp(i\gamma_5\theta_a\lambda_a/2)\psi$ and the scalar diquark condensates are partially rotated into pseudoscalar diquark condensates [13, 14]. For a K^0 mode the diquark condensates transform as [14]

$$\begin{aligned}
&\Delta^s_{22} \to \cos(\theta/2)\Delta^s_{22},\ \ \Delta^p_{25} \to i\sin(\theta/2)(\hat\theta_6 - i\hat\theta_7)\Delta^s_{22},\\
&\Delta^s_{55} \to \cos(\theta/2)\Delta^s_{55},\ \ \Delta^p_{52} \to i\sin(\theta/2)(\hat\theta_6 + i\hat\theta_7)\Delta^s_{55},\\
&\Delta^s_{77} \to \Delta^s_{77}, \qquad (10)
\end{aligned}$$

where $\theta = \sqrt{\theta_6^2 + \theta_7^2}$ and $\hat\theta_a = \theta_a/\theta$. In the same way Δ^s_{22} and Δ^s_{77} are partially rotated into Δ^p_{27} and Δ^p_{72} under a $\mathrm{K}^\pm$ transformation, while $\pi^\pm$ transformations rotate Δ^s_{55} and Δ^s_{77} into Δ^p_{57} and Δ^p_{75} [14]. According to the analysis in the chiral effective theory and confirmed numerically by Buballa [14] in the NJL model, the appearance of a pseudoscalar diquark condensate lowers the effective potential by [6]

$$f_\pi^2\mu_i^2(1-\cos\theta)^2/2, \qquad (11)$$

where $i = \mathrm{K}^0$, $\mathrm{K}^\pm$ or $\pi^\pm$ and $\cos\theta = M_i^2/\mu_i^2$.

So the CFL-K^0 phase is characterized by the CFL condensates plus two non-vanishing pseudoscalar diquark condensates Δ^p_{25} and Δ^p_{52}. Similarly, CFL-$\mathrm{K}^\pm$ and CFL-$\pi^\pm$ phases exist. Next to the CFL phase, different color superconducting phases are known, like the 2SC [26] (two-flavor color superconducting) phase ($\Delta^s_{22} \neq 0, \Delta^s_{55} = \Delta^s_{77} = 0$) and the uSC phase [27] ($\Delta^s_{22} \neq 0, \Delta^s_{55} \neq 0, \Delta^s_{77} = 0$). In the phase diagram we will present, we also encounter a phase with a Δ^s_{22} condensate together with a non-vanishing Δ^p_{52}. This phase we will call p2SC. A nonzero value of Δ^p_{52} can be obtained by an axial color transformation on the 2SC state. For convenience we have summarized the possible combinations in Table I.

phase	Δ^s_{22}	Δ^s_{55}	Δ^s_{77}	Δ^p_{25}	Δ^p_{52}	Δ^p_{27}	Δ^p_{72}	Δ^p_{57}	Δ^p_{75}
2SC	×	0	0	0	0	0	0	0	0
p2SC	×	0	0	0	×	0	0	0	0
uSC	×	×	0	0	0	0	0	0	0
CFL	×	×	×	0	0	0	0	0	0
CFL-K^0	×	×	×	×	×	0	0	0	0
CFL-$\mathrm{K}^\pm$	×	×	×	0	0	×	×	0	0
CFL-$\pi^\pm$	×	×	×	0	0	0	0	×	×
dSC	×	0	×	0	0	0	0	0	0
sSC	0	×	×	0	0	0	0	0	0
2SCus	0	×	0	0	0	0	0	0	0
2SCds	0	0	×	0	0	0	0	0	0

TABLE I: Definition of different phases. A 0 or a × denotes respectively a vanishing or non-vanishing condensate. If at least one of the quasi-particles has a gapless mode one writes a 'g' in front of the name of the phase, e.g. g2SC, gCFL, etc. If $\mu_Q > 0$, one speaks of CFL-K^+ and CFL-π^+, if $\mu_Q < 0$ of CFL-K^- and CFL-π^-. The five phases above the horizontal line appear in the phase diagram of neutral quark matter, Fig. 2. The other phases are possibilities (among others) which we have taken into account, but did not arise in the phase diagram.

To obtain the phase diagram of the NJL model under compact star constraints with the possibility of pseudoscalar condensation in the color-superconducting phases we will proceed as follows. In order to allow for electric neutralization, we introduce a free electron and muon gas and calculate the finite temperature (T) mean field effective potential which yields (see for example [9, 14])

$$\begin{aligned}
\mathcal{V} = {}& 2G(\sigma_u^2 + \sigma_d^2 + \sigma_s^2) + \frac{|\Delta^s_{AB}|^2 + |\Delta^p_{AB}|^2}{3G}\\
&- 4K\sigma_u\sigma_d\sigma_s - \frac{T}{2}\sum_{p_0 = \tilde\omega_n}\int\frac{\mathrm{d}^3p}{(2\pi)^3}\log\det S^{-1}\\
&- \frac{T}{\pi^2}\sum_{l=e,\mu}\sum_{\pm}\int_0^\infty \mathrm{d}p\, p^2 \log\left[1 + e^{-\beta(E_l \pm \mu_Q)}\right], \qquad (12)
\end{aligned}$$

where $\tilde\omega_n = (2n+1)\pi T$ and $E_l = \sqrt{p^2 + m_l^2}$. Weak equilibrium is automatically satisfied in this way (for example one can read off that $\mu_s = \mu_u + \mu_e$). Here we have assumed that neutrinos leave the star immediately. An analysis with neutrino trapping, as done for the phase diagram with scalar diquark condensates in Ref. [25], is left for future work. The electron and muon mass have the following values, $m_e = 0.511$ MeV and $m_\mu = 105.66$ MeV. The 72×72 matrix S^{-1} contains the inverse Nambu-Gorkov fermion propagator in the mean field approximation

$$S^{-1} = \begin{pmatrix} \mathbb{1}_c \otimes \mathcal{D} + \hat\mu \otimes \gamma_0 & t_A \otimes \lambda_B \otimes \Phi^1_{AB} \\ t_A \otimes \lambda_B \otimes \Phi^2_{AB} & \mathbb{1}_c \otimes \mathcal{D} - \hat\mu \otimes \gamma_0 \end{pmatrix}. \qquad (13)$$

Here

$$\mathcal{D} = \mathbb{1}_f \otimes (i\gamma_0 p_0 + \gamma_i p_i) - \hat M \otimes \mathbb{1}_d\ , \qquad (14)$$

and $\hat M = \mathrm{diag}(m_{0u} - 4G\sigma_u + 2K\sigma_d\sigma_s,\ m_{0d} - 4G\sigma_d + 2K\sigma_s\sigma_u,\ m_{0s} - 4G\sigma_s + 2K\sigma_u\sigma_d)$. The matrices Φ^1_{AB} and Φ^2_{AB} are equal to

$$\begin{aligned}
\Phi^1_{AB} &= \Delta^s_{AB}\gamma_5 + \Delta^p_{AB}\mathbb{1}_d, &(15)\\
\Phi^2_{AB} &= -\Delta^{s*}_{AB}\gamma_5 + \Delta^{p*}_{AB}\mathbb{1}_d. &(16)
\end{aligned}$$

The matrix $\mathbb{1}$ is the identity matrix in color (c), flavor (f), or Dirac (d) space.

To calculate the effective potential in an efficient way, one can multiply the matrix S^{-1} with $\mathrm{diag}(\mathbb{1}_c \otimes \mathbb{1}_f \otimes \gamma_0, \mathbb{1}_c \otimes \mathbb{1}_f \otimes \gamma_0)$ which leaves the determinant invariant. In this way, one obtains a new matrix R with ip_0's on the diagonal. We can write $R = ip_0\mathbb{1} + A$, where A is a Hermitian matrix independent of p_0. By determining the eigenvalues of the matrix A, one can reconstruct the determinant of S^{-1} for all values of p_0 which is $\prod_{i=1}^{72}(\lambda_i + ip_0)$. After summing over Matsubara frequencies, one finds

$$T\sum_{p_0=\tilde{\omega}_n} \log \det S^{-1} = \sum_{i=1}^{72} \left[\frac{|\lambda_i|}{2} + T \log\left(1 + e^{-|\lambda_i|/T}\right)\right]. \tag{17}$$

All that remains in order to determine the effective potential is to perform the integration over three-momentum p up to the ultraviolet momentum cutoff Λ numerically.

In order to enforce electric and color charge neutrality the following equations have to be satisfied

$$n_Q = -\frac{\partial \mathcal{V}}{\partial \mu_Q} = 0, \quad n_{3,8} = -\frac{\partial \mathcal{V}}{\partial \mu_{3,8}} = 0 \tag{18}$$

where n_Q is the electric charge density, and $n_3 = n_r - n_g$, and $n_8 = (n_r + n_g - 2n_b)/\sqrt{2}$.

The values of the condensates and the phase diagram are determined by minimizing the effective potential $\mathcal{V}$ with respect to the set of possible condensates. Together with the electric and charge neutrality constraints this implies that we have to solve the following equation

$$\frac{\partial \mathcal{V}}{\partial x_i} = 0, \tag{19}$$

where $x = \{\sigma_u, \sigma_d, \sigma_s, \Delta^s_{AB}\Delta^p_{AB}, \mu_Q, \mu_3, \mu_8\}$.

We will allow for the chiral condensates and the possible diquark condensates denoted in Table I. The analysis in the effective theory shows that the different phases with pseudoscalar condensation are separated by a first-order transition [6]. Therefore it is reasonable to minimize the effective potential with respect to the different possible sets of pseudoscalar diquark condensates separately. Thereafter one can compare the minimal values of the effective potential in order to determine the phase. This speeds up the numerical calculation.

Using the diagonal color transformations and the U(1) flavor transformations it is always possible to choose the scalar diquark condensates to be real, the phases of the pseudoscalar condensates however cannot be rotated away. We find that the effective potential of the NJL model with *real* CFL condensates and two pseudoscalar diquark condensates Δ^p_{25} and Δ^p_{52} is invariant under the transformation $\Delta^p_{25} \to e^{i\phi}\Delta^p_{25}$ together with $\Delta^p_{52} \to e^{-i\phi}\Delta^p_{52}$ (for the other possible sets of diquark condensates, the same transformation rule of course holds). This shows that one can always rotate one diquark condensate to be real. From Eq. (10) it follows that in the minimum of the effective potential the other diquark condensate is then real as well. We have also checked this numerically, by allowing for a complex pseudoscalar diquark condensate. Hence we can take the three scalar and the two pseudoscalar diquark condensates to be real. This speeds up the calculation as well.

To evaluate the derivatives of the effective potential (see also [11]) we have used the following formula

$$T\frac{\partial}{\partial x_j} \sum_{p_0=\tilde{\omega}_n} \log \det S^{-1}(x) = \frac{1}{2}\sum_{i=1}^{72} b_i \left(1 - \frac{2}{e^{|\lambda_i|/T} + 1}\right) \operatorname{sgn}(\lambda) , \tag{20}$$

where $b_i = (U^\dagger \partial A/\partial x_j U)_{ii}$. Here λ_i are again the eigenvalues of A, and U is a unitary matrix which contains in the i-th column the normalized eigenvector of A with eigenvalue λ_i. To obtain the complete derivative of the effective potential one still has to integrate Eq. (20) over momenta up to the cutoff Λ. The advantage of using Eq. (20) to evaluate the derivatives is threefold: firstly it is more accurate than the finite difference method, secondly it is also much faster since one had to diagonalize the matrix A anyway in order to obtain the value of the effective potential, and finally additional derivatives can be computed without much extra numerical work.

The speed of the calculation of the effective potential and its derivatives depends heavily on how fast one can compute the eigenvalues. There are several ways to speed up the calculation. Firstly, the determinant of A does not depend on the direction of $\vec{p}$. Therefore, one can choose $\vec{p}$ to lie in the z-direction. Together with the choice of the non-vanishing condensates mentioned above, this implies that A becomes a real symmetric matrix, which simplifies the calculation of the eigenvalues. Secondly, one can interchange rows and columns of A without changing its determinant. By doing so, one can bring A in a block-diagonal form. One can then determine the eigenvalues of the blocks separately which is significantly faster since the time needed to compute eigenvalues numerically scales cubically with the dimension of the matrix. In the most general case with two pseudoscalar diquark condensates, one can always reduce the problem to one 20×20 matrix and three 8×8 matrices.

We determined the eigenvalues using LAPACK routines [28]. The numerical integration over three-momentum p up to the cutoff was done using a Gauss-Legendre quadrature with 2×32 points at $T > 15$ MeV. For lower temperatures the Bose-Einstein distribution functions start to behave like step-functions, therefore the Gauss-Legendre quadrature, which is based on polynomial interpolation, becomes less accurate. For that reason we used Simpson integration with 256 points at lower temperatures. We have checked the accuracy of the integration procedures by doubling the number of integration points by 2. The condensates were determined by solving Eqs. (19) and (18) using a multidimensional rootfinding algorithm of the GSL package [29] with different initial conditions. The ground state was determined by picking the solution that has the lowest value of the effective potential. After the ground state was found we investigated the zeros of $|\lambda_i|$ as a function of momentum. If $|\lambda_i|$ has a zero, one of the quasi-particles has a gapless mode. In that case one speaks of the gCFL, g2SC, or guSC phase [30]. The problem of gapless phases are its chromomagnetic instabilities [31]. Therefore such a phase cannot be the phase with the lowest free energy.

IV. RESULTS

In this section we will discuss the phase diagram of quark matter under compact star constraints, that is electrically and color neutral matter in weak equilibrium. We will discuss two possible checks of our results. The first is to compare with the results of the chiral effective theory. The other is to compare with the phase diagram of Ref. [9] in which no pseudoscalar color-superconducting phases were taken into account.

We first present the phase diagram in the μ_B-μ_Q plane (so no electric neutralization) at $T = 0$. This allows for comparison with the chiral effective theory calculations of [6]. Thereafter we will discuss the phase diagram of neutral quark matter.

A. The μ_B-μ_Q phase diagram at $T = 0$

To predict the shape of the μ_B-μ_Q phase diagram one can use Eqs. (1) and (11). The resulting phase diagram is somewhat different from the analysis in the chiral effective theory of Ref. [6], because here electromagnetic corrections to the masses of the charged mesonic excitations have not been taken into account. Firstly, if μ_Q is positive, $\mu_{\mathrm{K}^+} > \mu_{\mathrm{K}^0}$ and $\mu_{\mathrm{K}^+} > \mu_{\pi^+}$. Since the energy gain of meson condensation is proportional to $\mu_i^2 - 2M_i^2 + M_i^4/\mu_i^2$ and $\mu_i > M_i$, it follows that the CFL-K$^+$ phase is favored over the CFL-K^0/π^+ phase for positive values of μ_Q. For negative values of μ_Q the CFL-K^0 phase is favored over the CFL-K$^-$ phase, because then $\mu_{\mathrm{K}^-} < \mu_{\mathrm{K}^0}$. So there has to be a phase transition from the CFL-K^0 phase to the CFL-K$^+$ phase at $\mu_Q = 0$. Secondly, if μ_Q is negative enough, pion condensation will be favored over neutral kaon condensation. Since M_K, M_π and μ_{K^0} are all proportional to $1/\mu$ the transition line should be proportional to $1/\mu$ as well at asymptotically high densities.

These conclusions are in agreement with the calculation of the phase diagram presented in Fig. 1. For $\mu_Q > 0$ we find the CFL-K$^+$ phase. There is a first-order phase transition at $\mu_Q = 0$. At negative μ_Q we encounter first the CFL-K^0 phase and then the CFL-π^- phase. If the baryon chemical potential is increased, the transition from the CFL-K^0 to the CFL-π^- phase occurs at smaller values of μ_Q, in agreement with the predictions.

We want to stress that, in order to calculate this diagram, we have used that chiral effective theory analysis [6] shows that the phase boundaries between the the phases with pseudoscalar condensation are first-order. Therefore, in order to simplify the calculation, we have assumed that this holds in the NJL model as well.

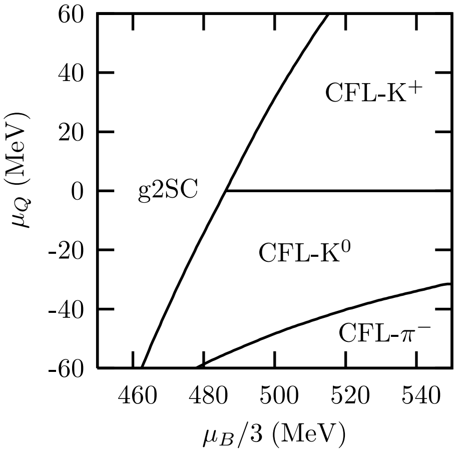

FIG. 1: The phase diagram of color neutral quark matter in weak equilibrium, as a function of baryon chemical potential and the electric charge chemical potential for $T = 0$. The solid lines denote first-order phase transitions.

The phase diagram of color neutral matter in weak equilibrium as presented in Fig. 1, does not necessarily contain all phases which are present in the phase diagram of matter that is also electrically neutral. This is because the electric neutrality constraint can force the electrically neutral system to be in a state which is a meta-stable state of color neutral matter in weak equilibrium.

B. The phase diagram of neutral quark matter

In Fig. 2 we have displayed our main result, the phase diagram of quark matter under compact star constraints, that is color and electrically neutral matter in weak equilibrium. This phase diagram was obtained by minimizing the effective potential on a grid of 440 (in the μ_B direction) by 300 (in the T direction) points. In this way we can determine the phase boundaries up to an accuracy of ± 0.25 MeV in the μ_B direction and ± 0.1 MeV in the T direction. After we minimized the effective potential on this grid we have checked the continuity of the minimum value of the effective potential.

In Fig. 3 we have displayed the values of the condensates and the chemical potentials in the minimum of the effective potential for $T = 0$ MeV, $T = 20$ MeV and $T = 40$ MeV. Outside the CFL phase, excellent agreement is found with [9] (their μ_3 and μ_8 differ by a factor 2 from ours due to another normalization). Since we took the pseudoscalar condensates to be real, a characteristic feature can be read off from Eq. (10), namely that they should have opposite sign. This we have indeed found and can be seen in our results in Fig.3.

The most important conclusion to be drawn from the phase diagram is that (for our realistic parameter choices)

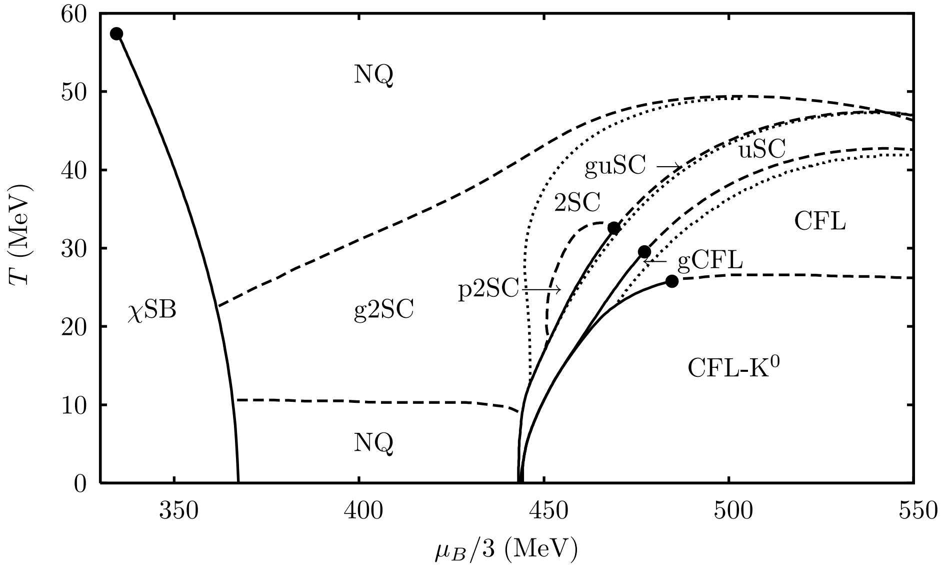

FIG. 2: The phase diagram of electrically and color neutral quark matter in weak equilibrium, as a function of baryon chemical potential and temperature. first-order phase transitions are denoted by a solid line, second-order phase transitions by a dashed line. The dotted lines indicate the (dis)appearance of gapless modes in the quasi particle excitation spectrum. Critical endpoints are denoted by a black dot. The χSB and the NQ labels denote the chirally broken and neutral chirally symmetric quark matter phases respectively. The definition of the color-superconducting phases can be found in Table I.

electrically and color neutral quark matter in weak equilibrium is at high baryon densities and low temperatures in the CFL-K^0 phase. We find that this phase contains no gapless modes, which implies that it does not contain chromomagnetic instabilities.

The CFL-K^0 is not always favored over the CFL phase. If at high baryon densities the temperature is raised the CFL-K^0 phase goes via a second-order phase transition to the CFL phase. At lower baryon densities we find a critical point where the transition to the CFL phase becomes first-order.

In electrically neutral quark matter, there should always be an excess of electrons and muons to compensate for the lower density of strange quarks compared to up and down quarks. Therefore μ_Q has to be necessarily negative (this can be seen in Fig. 3 as well), which implies that only the CFL-K^0 and the CFL-π phase could in principle be found in electrically neutral quark matter. We find the CFL-K^0 phase, but we do not encounter the CFL-π^- phase in the phase diagram.

Another striking feature of the phase diagram is the occurrence of the p2SC phase, a two-flavor color super conductor with a non-vanishing pseudoscalar diquark condensate, Δ^p_{52}. We find that the difference in free energy between the p2SC phase and the 2SC phase is exceptionally small. While usually a difference in the minimal value of the effective potential between two competing phases is in the order of $0.1 - 1$ MeV/fm^3, in this case it is only of order 0.1 keV/fm^3, see Fig. 4. Therefore it could well be that other parameter choices will let the p2SC phase disappear, but nevertheless it is very interesting that its free energy is so close to the ordinary 2SC phase.

We have displayed the values of the condensates of the p2SC phase in Fig. 5 again for $T = 30$ MeV. From this figure one can see that upon increasing the baryon chemical potential, one enters the p2SC phase via a second-order phase transition. The dotted line in the figure indicates the Δ^s_{22} condensate of the meta-stable 2SC phase. One can see from Fig. 5 that the Δ^p_{52} condensate has a relatively small value compared to the Δ^s_{22} condensate. We find that the square root of the sum of the values of the Δ^s_{22} and the Δ^p_{25} condensates is equal to value of the meta-stable Δ^s_{22} condensate. This shows that the p2SC phase can be obtained from the 2SC phase by an axial color transformation.

In our definition the p2SC phase contains a non-vanishing Δ^s_{22} and a Δ^p_{52} condensate. Using the off-diagonal color rotations, one can rotate a Δ^p_{52} in a Δ^p_{72} condensate. We have checked that taking into account a Δ^s_{22} and Δ^p_{72} condensate leads to the same phase diagram. We have also investigated whether other possible combination of Δ^p_{22}, Δ^p_{52} and Δ^p_{72} lead to a lower free energy, but we did not find such solutions with lower free energy.

We have also sought other possible combinations of two pseudoscalar diquark condensates and three scalar diquark condensates (of which one or more could potentially vanish), but we did not find any of them.

Comparing our results to the phase diagram of [9] (where the CFL-K^0 phase was not considered) we have good agreement outside the CFL-K^0 and the p2SC phase. The phase boundaries of the 2SC phase coincide. Also we find the boundaries of the g2SC and the guSC gapless

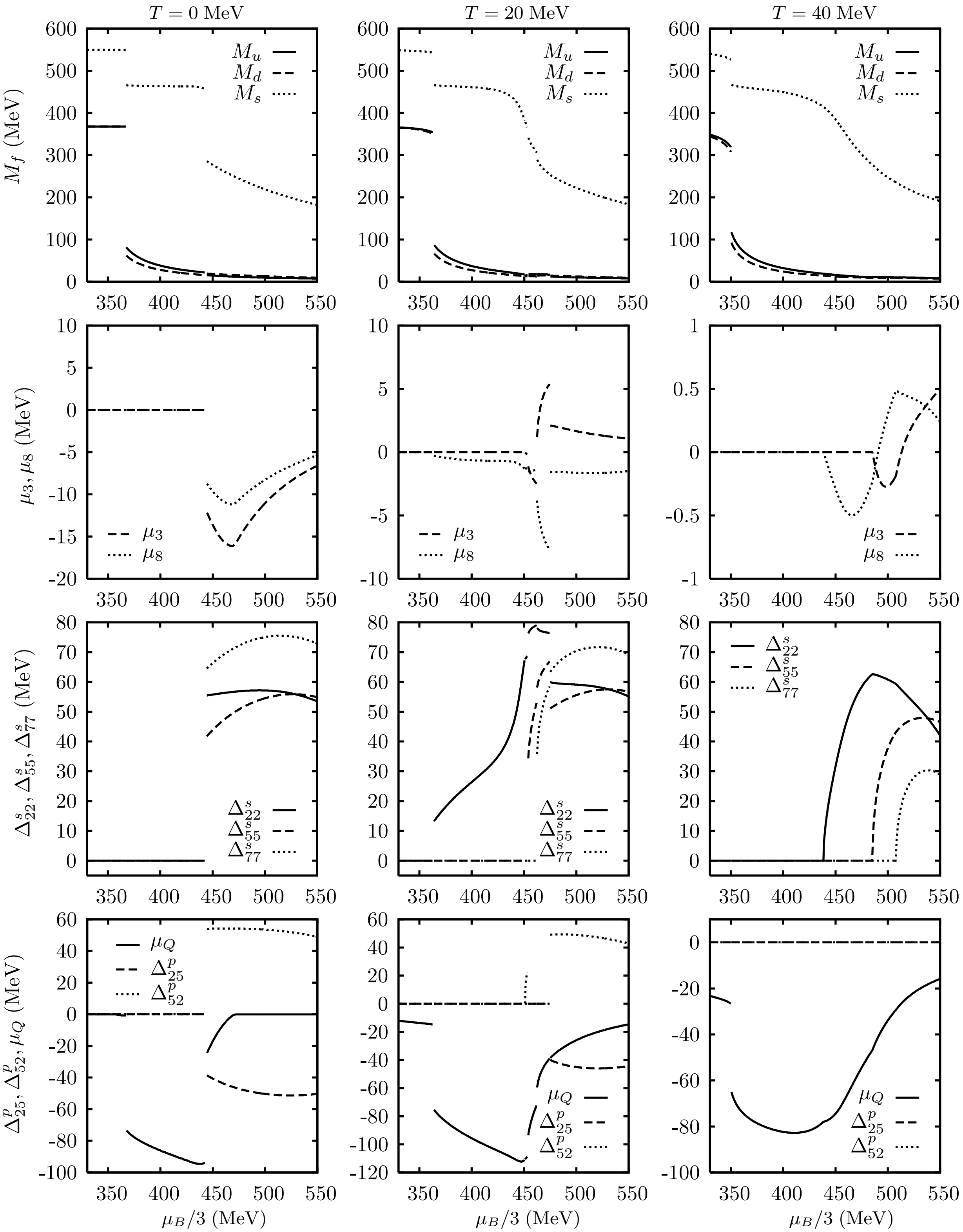

FIG. 3: Constituent quark masses, chemical potentials and condensates for electrically neutral quark matter in weak equilibrium. The constituent quark masses, chemical potentials and condensates are displayed as a function of baryon chemical potential, for $T = 0$ MeV (left-hand side), $T = 20$ MeV (middle panels) and $T = 40$ MeV (right-hand side).

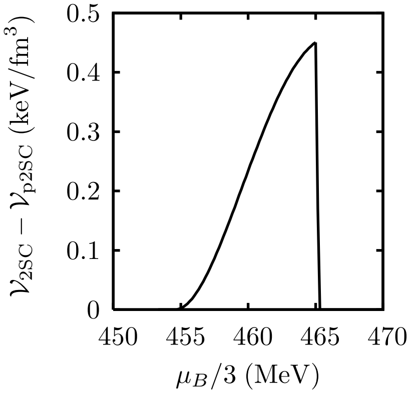

FIG. 4: The difference between the minimal values of the effective potential of the meta-stable 2SC phase and the p2SC phase for $T = 30$ MeV.

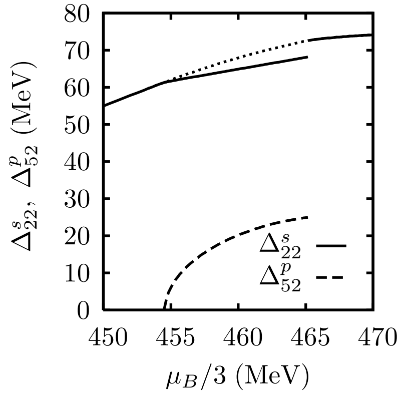

FIG. 5: The values of the condensates in the p2SC phase for $T = 30$ MeV. The dotted line indicates the meta-stable 2SC solution.

phases at the same place. At higher temperatures this also holds for the CFL and the gCFL phase boundaries (at lower temperatures we find the CFL-K^0 phase). Inspection shows that at zero temperature at $\mu = 443$ MeV there is a first-order transition from the neutral quark matter phase to the CFL-K^0 phase. This transition point is in excellent agreement with the calculations of [9] where at the same point a transition to the CFL phase was found. A difference is that we find that there is a very small window for the uSC phase, even for $T < 5$ MeV. Furthermore, our critical endpoints lie at somewhat higher temperatures.

It must be said that other sensible choices of parameters can lead to different phase diagrams (see e.g. [9] for a comparison). We however believe that the CFL-K^0 phase should be relatively stable against changing parameters. This does probably not hold for the p2SC phase, because of the very small difference in free energy between the p2SC and the 2SC phase. One must also be aware that in reality also crystalline phases [33] and phases with color-spin locking (see e.g. [32]) are possible. Also effects of non-local interactions could potentially modify the phase structure [34]. At low baryon densities, nuclear effects become important, which should also be taken into account (see e.g. [35] for a unified description of nuclear and quark matter in the NJL model).

Let us finally indicate some astrophysical consequences of the phase diagram displayed in Fig. 2 compared to the phase diagram obtained in [9] in which no CFL-K^0 phase was taken into account. In [9] the CFL-K^0 phase is replaced by a CFL and a gCFL phase. The difference in free energy between the CFL-K^0 and the CFL phase is not large, so the new phase may not have a huge influence on the equation of state and hence the mass-radius relationships of a compact star. However, the neutrino cooling of a star is very sensible to the low-energy excitations [36]. In phases without gapless modes, like the CFL-K^0 phase we found, the neutrino emissivity is exponentially suppressed compared to in phases with gapless modes [36]. Hence replacing the gCFL by the CFL-K^0 phase will reduce the cooling speed of a star with a quark core.

V. CONCLUSIONS

In this paper, we have calculated the μ_B vs. T phase diagram of electrically and color neutral quark matter in weak equilibrium, at high baryon densities. It could be useful for understanding compact stars with a quark matter core.

Our analysis has shown that neutral quark matter is in the CFL-K^0 phase at high baryon densities and low temperatures, rather thane the CFL phase. Other CFL phases with pseudoscalar condensation were not found. This CFL-K^0 phase is different from the ordinary CFL phase, since in the CFL-K^0 phase two pseudoscalar diquark condensates appear. The CFL-K^0 phase we obtained, contains no gapless modes. This implies that there are no chromomagnetic instabilities in the CFL-K^0 phase and that the neutrino emissivity is exponentially suppressed in the CFL-K^0 phase.

The CFL-K^0 phase does not completely replace the CFL phase. At higher temperatures we found a first and a second-order phase transition to the CFL phase.

Next to the CFL-K^0 phase, we found at intermediate densities and temperatures a 2SC phase which contains a pseudoscalar diquark condensate, which we have called p2SC. This phase can be obtained by an axial color rotation on the 2SC phase. The difference in the free energy between the 2SC and the p2SC phase is very small. This implies that corrections may let this phase disappear. In any case it would be interesting to have a more detailed investigation of this phase.

We have obtained good agreement with earlier calculations of the phase diagram were pseudoscalar condensation was not taken into account and with results from the chiral effective theory.

Acknowledgments

I would like to thank D. Boer and J.O. Andersen for useful discussions. Furthermore, I would like to thank D. Boer for valuable comments on the manuscript. The numerical calculations were performed on the Dutch National compute cluster Lisa, which is maintained by SARA computing and networking services.

[1] M. G. Alford, K. Rajagopal and F. Wilczek, Nucl. Phys. B **537**, 443 (1999).
[2] R. Casalbuoni and R. Gatto, Phys. Lett. B **464**, 111 (1999).
[3] D. T. Son and M. A. Stephanov, Phys. Rev. D **61**, 074012 (2000); [Erratum-ibid. Phys. Rev. D **62**, 059902 (2000)].
[4] T. Schäfer, Phys. Rev. Lett. **85**, 5531 (2000).
[5] P. F. Bedaque and T. Schäfer, Nucl. Phys. A **697**, 802 (2002).
[6] D. B. Kaplan and S. Reddy, Phys. Rev. D **65**, 054042 (2002).
[7] A. Kryjevski, D. B. Kaplan and T. Schäfer, Phys. Rev. D **71**, 034004 (2005).
[8] M. Buballa, Phys. Rept. **407**, 205 (2005).
[9] S. B. Ruster, V. Werth, M. Buballa, I. A. Shovkovy and D. H. Rischke, Phys. Rev. D **72**, 034004 (2005).
[10] D. Blaschke, S. Fredriksson, H. Grigorian, A. M. Öztaş and F. Sandin, Phys. Rev. D **72**, 065020 (2005).
[11] H. Abuki and T. Kunihiro, Nucl. Phys. A **768**, 118 (2006).
[12] F. Weber, Prog. Part. Nucl. Phys. **54**, 193 (2005).
[13] M. M. Forbes, Phys. Rev. D **72** 094032 (2005).
[14] M. Buballa, Phys. Lett. B **609**, 57 (2005).
[15] M. Alford and K. Rajagopal, JHEP **0206**, 031 (2002).
[16] K. Iida and G. Baym, Phys. Rev. D **63**, 074018 (2001); [Erratum-ibid. D **66**, 059903 (2002)]; A. W. Steiner, S. Reddy and M. Prakash, Phys. Rev. D **66**, 094007 (2002); A. Kryjevski, Phys. Rev. D **68**, 074008 (2003).
[17] M. Buballa and I. A. Shovkovy, Phys. Rev. D **72**, 097501 (2005).
[18] G. 't Hooft, Phys. Rev. D **14**, 3432 (1976); [Erratum-ibid. D **18**, 2199 (1978)].
[19] P. Rehberg, S. P. Klevansky and J. Hufner, Phys. Rev. C **53**, 410 (1996).
[20] D. T. Son and M. A. Stephanov, Phys. Rev. Lett. **86**, 592 (2001); J. B. Kogut and D. Toublan, Phys. Rev. D **64**, 034007 (2001).
[21] D. Ebert and K. G. Klimenko, arXiv:hep-ph/0510222.
[22] L. He, M. Jin and P. Zhuang, arXiv:hep-ph/0604224.
[23] A. Barducci, R. Casalbuoni, G. Pettini and L. Ravagli, Phys. Rev. D **69**, 096004 (2004); A. Barducci, R. Casalbuoni, G. Pettini and L. Ravagli, Phys. Rev. D **71**, 016011 (2005).
[24] H. J. Warringa, D. Boer and J. O. Andersen, Phys. Rev. D **72**, 014015 (2005), H. J. Warringa, arXiv:hep-ph/0512226.
[25] S. B. Ruster, V. Werth, M. Buballa, I. A. Shovkovy and D. H. Rischke, Phys. Rev. D **73**, 034025 (2006).
[26] D. Bailin and A. Love, Phys. Rept. **107**, 325 (1984); M. G. Alford, K. Rajagopal and F. Wilczek, Phys. Lett. B **422**, 247 (1998); R. Rapp, T. Schäfer, E. V. Shuryak and M. Velkovsky, Phys. Rev. Lett. **81**, 53 (1998).
[27] F. Neumann, M. Buballa and M. Oertel, Nucl. Phys. A **714**, 481 (2003).
[28] E. Anderson et. al., LAPACK User's Guide, Third Edition. SIAM, Philadelphia, (1999).
[29] M. Galassi et al. GNU Scientific Library Reference Manual, Second Edition, (2005).
[30] M. G. Alford, J. Berges and K. Rajagopal, Phys. Rev. Lett. **84**, 598 (2000); I. Shovkovy and M. Huang, Phys. Lett. B **564**, 205 (2003); M. Huang and I. Shovkovy, Nucl. Phys. A **729**, 835 (2003); M. Alford, C. Kouvaris and K. Rajagopal, Phys. Rev. D **71** 054009 (2005); K. Fukushima, C. Kouvaris and K. Rajagopal, Phys. Rev. D **71** 034002 (2005); M. Kitazawa, D. H. Rischke and I. A. Shovkovy, arXiv:hep-ph/0602065.
[31] M. Huang and I. A. Shovkovy, Phys. Rev. D **70**, 051501 (2004); R. Casalbuoni, R. Gatto, M. Mannarelli, G. Nardulli and M. Ruggieri, Phys. Lett. B **605**, 362 (2005); [Erratum-ibid. B **615**, 297 (2005)]; M. Alford and Q. h. Wang, J. Phys. G **31**, 719 (2005); K. Fukushima, Phys. Rev. D **72**, 074002 (2005).
[32] D. N. Aguilera, D. Blaschke, M. Buballa and V. L. Yudichev, Phys. Rev. D **72**, 034008 (2005).
[33] M. G. Alford, J. A. Bowers and K. Rajagopal, Phys. Rev. D **63**, 074016 (2001).
[34] D. Gomez Dumm, D. B. Blaschke, A. G. Grunfeld and N. N. Scoccola, arXiv:hep-ph/0512218.
[35] S. Lawley, W. Bentz and A. W. Thomas, J. Phys. G **32** 667 (2006).
[36] T. Schäfer and K. Schwenzer, Phys. Rev. D **70**, 114037 (2004).